

**Optical Imaging in Biology and Medicine**  
**Master in Photonics & Europhotonics Master Program**

# Adaptive Optics for Microscopy

Carles Otero Molins

Johannes Rebling

December 7, 2013

## **Abstract**

To achieve optimal, diffraction limited images with the best possible resolution has always been a challenging topic and an important goal in science and in biophotonics in particular. Although many new techniques to acquire superresolution images were developed in the last decade, unwanted aberrations often still compromise the resolution and brightness of the images taken with these techniques. Adaptive Optics (AO), a technique originated from astronomy, is a possible solution to compensate for aberrations in biomedical imaging.

This report have presented a review of the numerous applications of AO applied to modern microscopy methods. We have reviewed the basic principles of AO, described how the aberration information is obtained (via direct and indirect sensing) and how AO is applied in the main microscopy techniques (widefield and point scanning techniques). We have shown that AO methods have been applied in almost all modern microscopy techniques. However, the increase in resolution and signal intensity depends strongly on both the AO system and the microscopy technique, thus, great care has to be taken when trying to implement the optimal AO technique.

## **Contents**

<b>1</b>	<b>Introduction</b>	<b>1</b>
<b>2</b>	<b>Aberration Measurement and Correction</b>	<b>1</b>
2.1	Direct Wavefront Sensing . . . . .	2
2.2	Indirect Wavefront Sensing . . . . .	4
2.2.1	Stochastic Optimization . . . . .	5
2.2.2	Model Based Optimization . . . . .	6
2.3	Aberration Correction . . . . .	6
<b>3</b>	<b>Adaptive Optics Methods applied in Microscopy</b>	<b>7</b>
3.1	Widefield Microscopy . . . . .	7
3.1.1	Direct Wavefront Sensing in a Fluorescence Microscope . . . . .	8
3.1.2	Indirect Wavefront Sensing in a Transmission Microscope . . . . .	9
3.1.3	Structured Illumination Microscopy . . . . .	10
3.2	Point Scanning Microscopes . . . . .	12
3.2.1	Confocal Microscopes . . . . .	12
3.2.2	Indirect Wavefront Sensing in Multiphoton Scanning Microscopy . . . . .	13
3.2.3	Direct Wavefront Sensing in Two Photon Florescence Microscopy . . . . .	15
<b>4</b>	<b>Conclusion &amp; Future Prospects</b>	<b>16</b>
<b>References</b>		<b>17</b>

## 1 Introduction

It is well known that optical aberrations degrade the resolution and brightness of images. This results in a reduction of both lateral and axial resolution and a decrease in signal intensity. In general aberrations can be defined as the wavefront distortions with respect to an ideal sphere. These distortions can be caused by imperfections and inhomogeneities in any part of the optical system. In microscopy, aberrations may arise from the microscope itself or the specimen under study [1]. Aberrations always limit the final image quality and can vary from one specimen to another. In this case they can not be corrected by an optimized optical design which makes a dynamic correction necessary.

It is of little surprise that scientists have been trying to overcome this problem for many years, an effort that resulted in what nowadays is called Adaptive Optics (AO). The first proposal of the use of AO technology was suggested in the year 1953 in the context of astronomical optics for the compensation of the aberrating effects of the atmosphere [2]. The main idea of AO is the modulation of an incoming wavefront in such a way that we can record an image without aberrations. It is based upon the principle of phase conjugation: the correction element introduces an equal but opposite phase aberration to that present in the optical system. In order to do that, we need to be able to measure these distortions reliably. The most direct way is to use a wavefront sensor, such as the Shack-Hartmann [3, 4]. Also, interferometric techniques have been used to measure aberrations [5]. Furthermore, there are indirect or sensorless methods in which aberrations are determined using an optimization algorithm and do not employ a direct wavefront sensing [6]. A control system then processes the aberration information and uses it to control an adaptive correction element. The adaptive element is needed to modulate and correct the incoming wavefronts before the light reaches the imaging detector. This task is usually performed by a deformable mirror or a liquid crystal spatial light modulator (LC-SLM).

Although Adaptive Optics systems have been successfully introduced in applications such as astronomy, laser beam shaping, optical communications, data storage and ophthalmology [7], it is not trivially applied to microscopy. One particularly difficult problem in AO microscopy is how the aberration information is obtained in each of the different microscopy techniques, since direct sensing is not usually easily implemented as it is the case of astronomy.

Optical microscope techniques can be divided in two main groups: the widefield techniques and the point scanning techniques. Examples of the first group are the conventional transmission microscopy, the structured illumination microscopy and the fluorescence microscopy. Some point scanning techniques are the confocal microscopy, Stimulated Emission Depletion (STED) or the non-linear microscopy such as Two-Photon Excitation Fluorescence (TPEF), Second Harmonic Generation (SHG) microscopy, Third Harmonic Generation (THG) microscopy and Coherent anti-Stokes Raman (CARS).

In order to explain how adaptive optics and microscopy are linked together, we will start explaining the basis of adaptive optics. This includes a brief review of the concept of aberrations and how they are most commonly characterized. After that, we will explain in more detail the main methods for wavefront sensing, the main aberration corrector devices. Furthermore, we will show some applications of the AO in different widefield and point scanning microscopy techniques. The last part will be a short explanation of future prospects and conclusions.

## 2 Aberration Measurement and Correction

In practice, no optical system can be totally free from aberrations. That means that all the rays originating from the same object point and going through an optical system will not converge into the same point at the image plane. In other words, the wavefront is distorted with respect to an ideal one when passing through a real system. Thus, we can define the wavefront aberration function as the optical path difference between the aberrated (real) wavefront and the reference (perfect) wavefront. These aberrations can be introduced both upon reflection from a non-planar irregular surface and by passing through an inhomogeneous media as shown in Fig. 1.

In biological microscopy, the two potential sources of aberrations are the optics and the specimen under study. Regarding the optics, one important parameter is the Numerical Aperture (NA), a higher

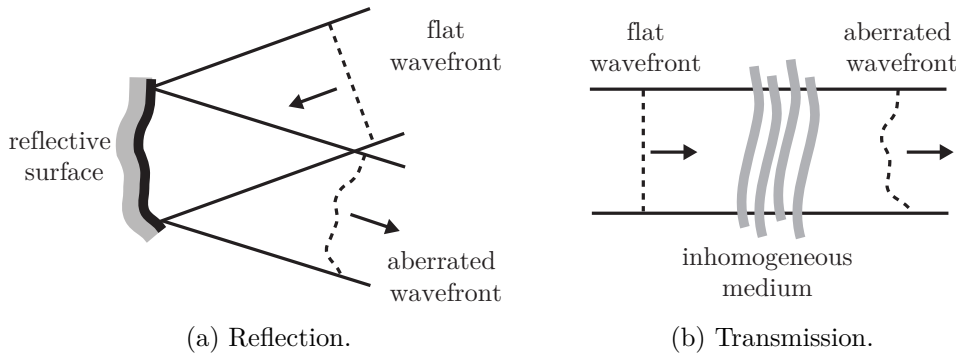


Figure 1: Wavefront aberrations due to (a) reflection from a non-planar surface and (b) caused by propagation through a non-uniform refractive index distribution [1].

NA not only increase theoretically the resolution but also aberrations become more significant. Besides, aberrations might also come by the difference of refractive index between the microscope coverslip and the specimen mounting medium. Regarding the specimen, aberrations are mainly caused by the variations in refractive index due to the three-dimensional nature of cells and tissue structures. These sample induced aberrations generally become dominant when the image focus lies deep within the sample, since light has to pass a large distance through an inhomogeneous medium [1].

There are different ways to characterize the aberrations mathematically. In systems with circular symmetry (circular apertures) it is very common to use the Zernike polynomials because they form a complete, orthogonal set of functions defined over a unit circle [8]:

$$W(\rho, \phi) = \sum_n^k \sum_{m=-n}^{m=n} c_n{}^m Z_n{}^m(\rho, \phi), \quad (2.1)$$

where  $W(\rho, \phi)$  is the wavefront aberration function in polar coordinates at the exit pupil,  $c_n^m$  are the Zernike coefficients and  $Z_n^m(\rho, \phi)$  are the Zernike modes (or polynomials). As we can see in the equation, the wavefront aberration function is a linear combination of polynomials. Therefore, the more polynomials (i.e. modes,  $Z_n^m(\rho, \phi)$ ) we can measure, the better characterization of the  $W(\rho, \phi)$  function we have. Representing aberrations in this way can simplify the design, control and characterization of the Adaptive Optics system specially due to the independence of each polynomial with respect the others. This powerful property is given by the orthogonality.

Although it is known where the aberrations come from, it is not always easy to measure them and implement the measure inside the optical system. There are different classifications of wavefront sensing in the bibliography [9]. Here we will use the one employed by *Martin J. Booth* [1] and we will explain the most common methods of wavefront sensing applied to microscopy.

## 2.1 Direct Wavefront Sensing

Direct Wavefront Sensing is based on a direct measure of the phase gradient or the wavefront slope, it is considered as an aperture-plane sensing. Within this group there are several techniques such as interferometric, although in general the most used is the Shack-Hartmann.

The Shack-Hartmann technique is based on a two-dimensional array of lenslets -a matrix of microlenses-all with the same diameter and the same focal length. When an incoming beam goes through the matrix gets split and multiple focal spots are recorded onto the detector, which is placed at the focal plane of the microlenses, as shown in Fig.2. The recording device is usually a CCD camera and typical microlens diameter range from about 100 to 600 mm with typical focal lengths ranging from a few millimeters to about 30 mm [10]. By measuring the displacements with respect the optical axis ( $\Delta x, \Delta y$ ) of each focal spot (Fig. 2) it is possible to reconstruct the wavefront slopes and finally to obtain the wavefront aberration function. It is important to take into account that this technique loses its accuracy for strong aberrated wavefronts, mainly due to overlapping of focal spots or crossover.

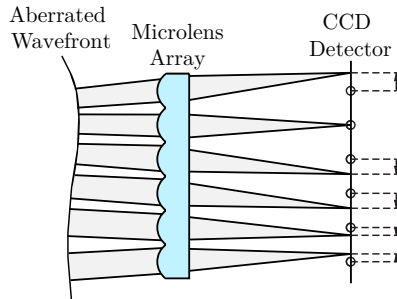


Figure 2: Two-dimensional section of Shack-Hartmann matrix of microlenses. An incoming beam is divided and imaged onto a CCD detector. This generates separate focal spots for each microlens. If the wavefront is not aberrated, each spot will be placed along the central axis of each microlens. If it is aberrated, it will be displaced with respect to this axis and a wavefront reconstruction can be performed based on the magnitude and direction of this displacement. Image after [11].

While the basic idea of this sensing techniques is simple, we must note that a well defined wavefront in the pupil of the system is required, which can only be produced by a point-like emitter. When studying three-dimensional, biological specimens, a single point-like emitter is usually not encountered which leads to a number of problems. The first one is the superposition of wavefronts coming from the light in the focal region and the light out-of-focus. These superposition depends on the coherence of the emitted light. Coherent light will cause interference in the pupil, thus causing ambiguous sensor readings rendering the measurement useless for aberration correction. Also, another problem that can arise is that the sensor might detect more signal intensity from the light out-of-focus rather than the light from the focal region. In order to overcome this situation, a spatial filter between objective and sensor can be used, much like the pinhole used in confocal microscopy. It is also possible to use coherence gating to exclude out-of-focus light instead of the spatial filter, although it is a more complex method [12].

However, if the specimen behaves as a point-like emitter, it still needs some restrictions in order to apply direct sensing. That is because if coherence light is used and the specimen has a planar-mirror behavior in the focal region, the sensor will just be able to measure twice the even components of the aberrations produced in the illumination path (or emission path). This is due to the spatial inversion caused by any mirror and the interference between the illumination and emission wavefronts, as shown in Fig. 3). Hence we lose information about aberrations and indirect sensing schemes should be preferred. But if the specimen behaves as a point-like scatterer, it will emit incoherent light and the sensor will measure the aberrations produced in the emission path. In this case direct sensing can be applied.

Nowadays, the most common approaches of direct sensing to microscopy are the use of Two Photon Excitation Fluorescence (TPEF) technique or the use of fluorescence microspheres. In the first one, microscopists take advantage of not only the incoherent emission due to the fluorescence process but also of the light confined in the focal region due to the nonlinear process. Therefore, a point emission is present and it is possible to apply direct sensing. More details can be found in section 3.2.3. Another approach is to create a point-like scatterer, a fluorescent microsphere, and insert it into the sample. These microspheres are treated beads capable of emitting in different colors such as blue, crimson, red, orange, green or yellow, resistant to different conditions and with diameters that more or less go from 0.01 to  $4\mu\text{m}$ . They can be engineered to target different biological tissues and there are several ways to insert these microspheres into the sample such as negative pressure injection, pressure injection, matrotrophically or diffusion. Since they are loaded with fluorescent dyes, an excitation beam is needed to activate the fluorescent emission. This may be taken into account if direct sensing is applied to fluorescence microscopy. In this case, two excitation beams and two detection devices need to be used. One beam is needed for the wavefront sensing, linked with the fluorescence of the microsphere, and one for imaging the sample. Another important characteristic about this method is related with

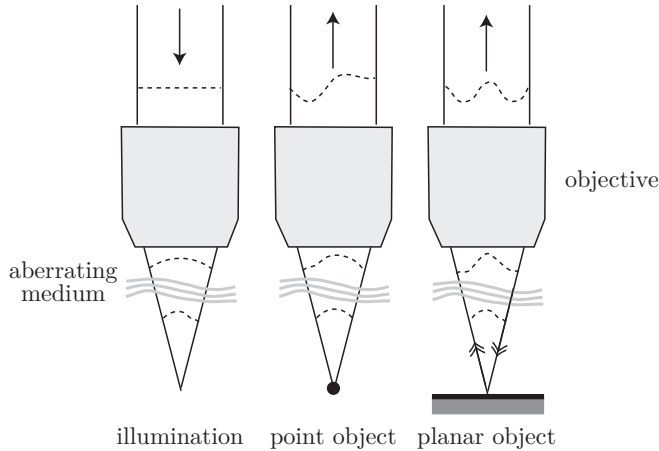


Figure 3: Representation of the two effects due to the specimen structure on wavefront measurements.

The left figure shows how the wavefront is aberrated in the illumination path. In the center it is shown a point-like scatterer. Only the emission path is measured. In the right figure it is shown a planar reflector. The illumination wavefront is spatially inverted on reflection before acquiring further aberration in the emission path. Image after [1].

the microsphere density and localization. Once the beads are inserted into the sample it is not possible to control their distribution or positions, thus, a certain density of microspheres is necessary in order to cover enough sample for sensing. Although it is an invasive method and seems to add more complexity to the system, *Azucena et al.* showed that it is possible to apply direct sensing in biological microscopy using these microspheres [13]. They showed that a micron fluorescent microsphere provides enough light to run the AO system loop at 10 ms bandwidth, and even having multiple microspheres relatively close to each other, either in the same focal plane or in different planes, does not present a problem if a confocal illumination is used. However, regarding the microsphere density, further investigations are required to know what are the limits of the amount of microspheres that can be used for sensing and without photodamaging the sample. More information about the applications of this method can be found in section 3.1.1 and 3.2.1.

## 2.2 Indirect Wavefront Sensing

While direct wavefront sensing techniques are widely applied in astronomy, they are less common in microscopy techniques. This is mainly because it is not easy to find a “guide-star”<sup>1</sup> (point emitter) in a biological specimen. If there are no features in the specimen that occur naturally and which resemble a point source, one has to implement them manually which might alter the function of the specimen or might even be toxic to the sample. Besides, modern microscopes are also highly complex and optimized, which makes it difficult to insert a relatively large wavefront sensor. For samples with weak signal strength, it is also desirable to collect as many photons as possible for the imaging process. Splitting the beam and using part of the light emitted from the sample for direct wavefront sensing might hence decrease the signal strength.

Indirect techniques do not measure the wavefront directly but instead optimize some merit function (also called quality metric) that depends on the optical system. Indirect methods are used more often in industrial and medical applications. They usually require very little additional hardware. Once the technique is optimized for a specific problem, indirect schemes are easier to implement in practice and are more prone to errors due to the lack of additional hardware (a single deformable mirror might be sufficient to implement adaptive optics in an existing microscope).

For these techniques, the optimization of an image quality metric is mainly a mathematical rather than a technical problem. The aberration correction is performed through an iterative optimization of

<sup>1</sup>The term “guide star” is used in reference to astronomy. There a star or a laser spot projected in the sky is used as the point emitter for sensing.

an image quality metric. The metric is usually based on spatial frequencies [14] or image intensity [15] and gives a mathematical measurement of how “good” the recorded image is. In many practical systems aberrations can be accurately represented by a small number of modes of an orthogonal basis, such as Zernike polynomials. The optimization is then performed by adapting the polynomial coefficients applied to the deformable mirror either stochastically or by using an appropriate mathematical model. A general overview of the method is shown in Fig. 4.

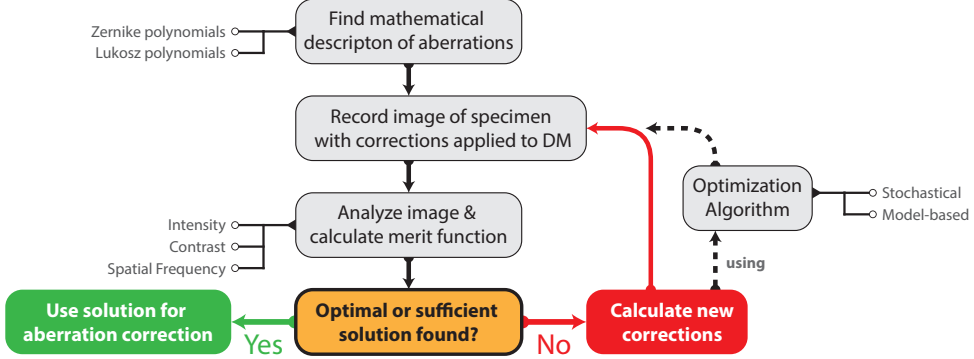


Figure 4: General description of the steps neccesary to perfrom indirect wavefront sensing.

### 2.2.1 Stochastic Optimization

Several stochastic algorithms, such as hill climbing (HC), genetic (GA) and random search (RS) exist. Wright *et al.* [16] compared these algorithms in terms of repeatability and reliability of the solutions, the final axial resolution of the system and the time taken to complete an optimization. They explain how the different algorithms can be useful, concluding that GAs have the best potential to achieve an optimal solution of the optimization process. In the context of adaptive-optical control, the genetic algorithm is well-suited because of its ability to independently optimize many variables at once [17]. It is for that reason, that genetic algorithms are one of the most popular stochastic optimization algorithms. They try to find an optimal solution by simulating an evolution process, and the important steps are shown in Fig. 5.

The basic idea of GAs is to create a population of individuals, also called chromosomes. In the case of AO, each chromosome corresponds to a specific shape of the deformable mirror. The chromosomes either represent the set of voltage applied to each actuator of the DM or, more commonly (due to its preferable optimization performance [18]), representing the set of the Zernike polynomial coefficients. After creating this initial population, each individual is evaluated and assigned a fitness value using the image quality metric. Mirror shapes, i.e. individuals, with a better fitness are closer to the optimal shape. The GA tests the entire population of individuals and selects a percentage of the most fit individuals to become parents for the next generation, called intermediate population. Then, recombination and mutation are applied to the intermediate population to create the next population. This new generation is tested again, repeating the above steps. The evolution process stops when the population includes a sufficient (or better optimal) solution. By going through this procedure, the GA gradually finds the optimal mirror shape that will yield the best solution of the quality metric. GAs do not require any preliminary information about the system but they are more time consuming than model-based approaches. Genetic algorithms are highly complex and have a large set of parameters that influence the optimization process. Those parameters are the size and randomness of initially population, the mutation and crossover rates, the size and selection of intermediate population as well as many more. A detailed description of the underlying principles and the separate steps can be found in [19] while an example where a genetic optimization algorithm is used is presented in section 3.2.2

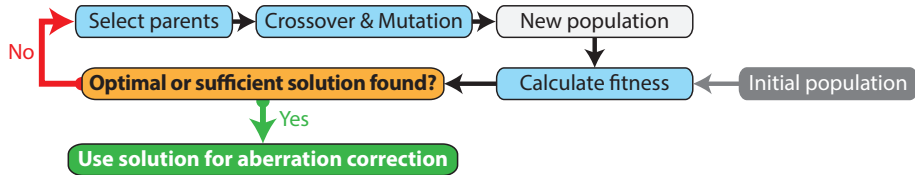


Figure 5: Overview of a genetic algorithm.

### 2.2.2 Model Based Optimization

Methods based on a mathematical model acquire a sequence of images, each with a different, predefined aberration applied. The correction aberration is estimated from the information in these images and this process is repeated until the image quality is considered acceptable. The number of measurements needed to obtain an acceptable image depends strongly upon the optimization algorithm, the parameters used, the mathematical representation of the aberration and the object structure. For the earliest and most generic algorithms the number of measurements per aberration mode increases quadratically or exponentially with  $N$ , the number of corrected aberration modes [20]. The so called direct maximization method (as described in Section 3.1.2) is significantly more efficient, requiring only  $2N+1$  measurements for  $N$  modes. With this technique, Lukosz polynomials [21] are used to classify the aberrations. The effects of different modes can then be separated and the optimization of each mode becomes independent and hence more efficient.

An effective model-based adaptive optics scheme should also be independent of the imaged object and should permit the separation of aberrations and object influences on the measurements. This separation is also possible through the appropriate choice of optimization metric and aberration representation [14]. The interested reader will find more information on the mathematical background in reference [14, 20, 21, 22].

### 2.3 Aberration Correction

The wavefront correctors are an essential part of an adaptive optics system. The goal is to apply a certain phase profile to the incident wavefront by changing either the physical length over which the wavefront propagates or the refractive index of the medium through which the wavefront goes. Wavefront correctors are built using either mirrors or liquid crystals. The former apply the phase change by adjusting their surface shape (i.e., change their physical length while keeping the refractive index constant) while the latter keep the physical length constant and rely on localized changes in refractive index. Mirror-based correctors are wavelength and polarization independent and can be reconfigured at rates of a few kilohertz [1]. They can have a continuous surface (i.e., discrete actuator, bimorph or membrane mirrors) or segmented surface (i.e. piston-only or piston/tilt mirrors) as shown in Fig. 6. Unlike continuous mirrors, the segmented mirrors have gaps between the segments that reduce the efficiency and quality of the correction, although they can achieve much better wavefront fitting.

Liquid crystal-based modulators change the refractive index electronically or optically, are wavelength and polarization dependent and can reach velocities of just a few tens of hertz. The nematic liquid crystal is the most common for AO applications. In general, they are much cheaper than the mirror-based correctors, are capable of producing more complex phase patterns but they have lower light efficiency due to absorption.

In AO microscopes the first choice in most cases is the deformable mirror because of the higher light efficiency and velocity. Furthermore, they are better suited for fluorescence techniques due to their polarization independent behavior. However, in particular cases, liquid-crystal modulators can be sufficient if aberration correction is only needed in the illumination path.

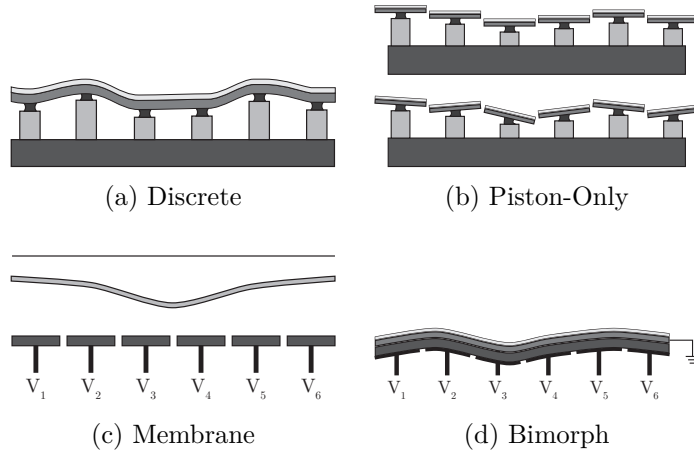


Figure 6: The four main mirror correctors. (a) Discrete actuator deformable mirrors consist of a continuous, reflective surface and an array of actuators, each capable of producing a local deformation in the surface. (b) Piston-only segmented correctors consist of an array of small planar mirrors whose axial motion (piston) is independently controlled. Piston/tip/tilt-segmented correctors add independent tip and tilt motion to the piston-only correctors. (c) Membrane mirrors and (d) Bimorph mirrors. Image after [10].

### 3 Adaptive Optics Methods applied in Microscopy

Adaptive optics techniques have found their way into almost all kinds of modern, high resolution microscopy techniques. These microscopes have been combined with direct wavefront sensing and sensorless AO, using deformable mirrors or spatial light modulators for aberration compensation (all of which have been described in Section 2). This includes standard widefield microscopes as well as highly sophisticated and specialized point scanning methods such as CARS and Stimulated Emission Depletion (STED) techniques. It has to be noted however, that some of these methods are themselves only a few years old. Therefore, they are still being optimized and so are the AOM techniques. It is an interesting field of research with new ideas being implemented every year.

AO was first used in confocal and two-photon fluorescence microscopy, both of which are commonly used in biomedical applications. These microscopes suffer from a significant drop in signal and resolution as the focus is moved deeper into the specimen, which is caused by aberrations [23].

AOM is also used for imaging of live specimens. Due to an increased excitation signal and improved light collection from the specimen, acquisition times can be reduced and contrast can be enhanced. Techniques that without AO are too slow for live imaging might now be usable, opening up completely new fields of research. Another advantage of AO lies in the microscopy design. Using AO methods, can help the designer to relax the aberration tolerance. This permits a significant reduction in the complexity of the optical system while maintaining diffraction limited operation.

This section will describe, using state of the art examples how AO is implemented in both widefield and point scanning systems.

#### 3.1 Widefield Microscopy

As mentioned above, AO techniques are being applied in widefield microscopy. In conventional microscopes, widefield illumination is provided using back light illumination or in the case of reflection or fluorescence modes, via the objective lens. The image quality depends only on the aberrations induced in the detection path and is independent of the aberrations of the illumination path. Aberration correction is therefore only necessary in the detection path and a single pass adaptive optics system will suffice [24]. Hence, the goal of AO for widefield microscopy is to restore the best possible imaging and to correct for aberrations induced both by an imperfect imaging system as well as by the imaged specimen. The latter becomes more important for thick biological samples where the light has to travel a larger distance through a medium with an inhomogeneous refractive index.

Many other highly specialized widefield microscopy techniques have been developed and for most of those, AO schemes for aberration correction and resolution optimization have been presented. Three widefield microscopy techniques will be presented in this section, starting with the implementation of direct wavefront sensing for a fluorescence microscope in section 3.1.1. The implementation of AO in a standard transmission microscope using a sensorless wavefront sensing scheme is explained in section 3.1.2) and finally, how the theoretical background of this technique can be applied to more sophisticated microscopy schemes is then shown on the example of structured light illumination (Section 3.1.3), a specialized wide field technique.

### 3.1.1 Direct Wavefront Sensing in a Fluorescence Microscope

While indirect sensing has several advantages over direct sensing (see sec. 2.2), they have one important drawback that can ultimately not be overcome. They all depend on an iterative optimization procedure to estimate and correct for the aberrations. While random optimization requires many iterations (in some cases up to 3000 iterations per mirror actuator [25]) other methods base the iterations on complicated models and are able to achieve indirect sensing with as little as  $2N + 1$  iterations (where  $N$  is the number of corrected aberration modes) [14, 26, 27]. However, even these methods require the sample to be exposed and imaged multiple times. While this is suitable for some systems such as CARS where photobleaching is not an issue, it often limits the feasibility of AO in other imaging techniques. Model based indirect schemes are also inflexible, since the model used for the optimization is depending on both the imaging system and the sample. Another different approach is to use fluorescence microspheres for a direct wavefront sensing scheme, explained in section 2.1 and presented by *Azucena et al.* in 2010 [13]. Until their publication, most AOM system only measured the wavefront indirectly due to the added complexity and the lack of natural point-source references such as the “guide-stars” used in astronomy and vision science. The authors overcome the latter problem by introducing a suitable fluorescent point source reference beacon as an artificial guide-star into a sample of *Drosophila* embryo [28]. They injected crimson beads (fluorescence microspheres) of ( $1\text{ }\mu\text{m}$  diameter). A Shack-Hartmann sensor and a deformable mirror were used. In order to separate the fluorescence of the microspheres from the fluorescence of the sample they implemented two different channels, that is, two illumination beams and two detectors (see Fig. 7). The wavefront measurement and correction channel was characterized by an excitation beam at 632.8 nm and the sample’s excitation was at 448 nm. We must note that the peak emission of the fluorescence microspheres was at 647 nm and for the sample’s fluorescence was at 510 nm. Therefore, they could image both signals separately. Furthermore, they introduced additional filters to improve this separation.

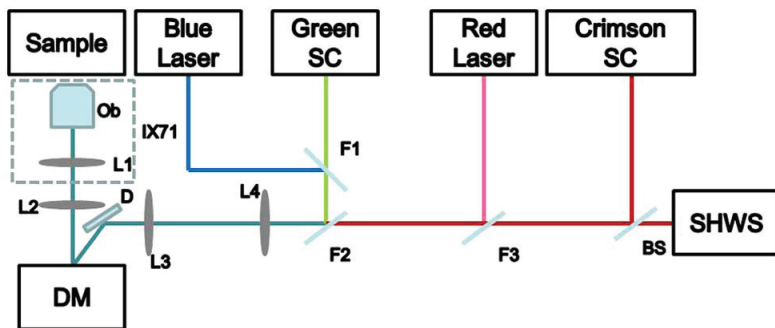


Figure 7: AO fluorescence microscope setup. The blue laser and the green camera correspond to the imaging channel of the sample. The red laser and the crimson camera correspond to measurement and correction channel [28].

The final data analysis of *Azucena et al.* demonstrated that their approach can improve the resolution for an image gathered at 510 nm even though the wavefront measurement and correction is made at 647 nm. This is due to the fact that the wavefront sensor measures the change in optical path difference, which does not vary significantly over a large portion of the visible spectrum [28]. Figure 8) shows a clear improvement in resolution. The microspheres imaged can clearly be distinguished when the adaptive

optics system is used, as shown in Figure 8b. The same image, taken without AO has a much lower resolution and microspheres that are close to each other can not be distinguished, as shown in Figure 8a.

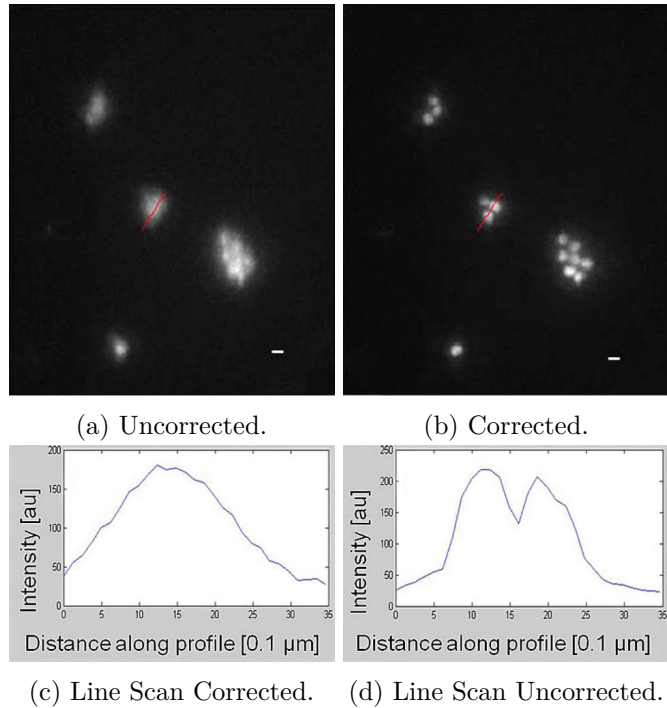


Figure 8: Imaging of microspheres. In (a) with AO system deactivated, (b) with active AO system. (c) shows the intensity profile of the red line shown in (a). (d) shows the intensity profile along the same line with active aberration correction. The white line is approximately  $1\text{ }\mu\text{m}$  in length. A clear improvement in resolution can be observed when AO is applied during the imaging process in both the images and the intensity profile. The image in (a) suggest a single, large microsphere while (b) shows, due to the better resolution, that one actually observes three microspheres [28].

### 3.1.2 Indirect Wavefront Sensing in a Transmission Microscope

To implement adaptive optics with standard (incoherent) transmission microscopes, *Debarre et al.* [14] implemented an indirect, sensorless and image-based adaptive optics scheme. As described earlier in Section 2.2, image-based techniques do not require an additional wavefront sensor but retrieve the correction data directly from the recorded images. Hence the authors used a standard microscope for AOM by simply adding a deformable mirror in the beam path (see [14] for experimental setup). As with all indirect sensing schemes, the difficulty is to find a good metric for image quality, which allows to determine the appropriate correction parameters. The presented method uses low spatial frequency content of the image as the optimization metric. The aberration is represented in terms of Lukosz modes which are based on Zernike polynomials. The presented technique consists of modeling the effects of aberrations on the imaging of low spatial frequencies, which Lukosz modes are found to be ideal for. By modeling the aberrations as a series of Lukosz modes they develop an optimization metric as the sum of a range of low spatial frequencies. The optimization function is related to the coefficients of the aberration expansion by a Lorentzian function. The aberration correction process is then performed as the maximization of the Lorentzian. Due to its paraboloidal maximum, the use of simple maximization algorithms is possible. Furthermore, the authors show that the optimization can be performed as a sequence of independent maximizations for each aberration coefficient.

The correction process is shown in Figure 9 for the correction of a single Lukosz mode using a scatterer specimen. Using the deformable mirror (DM), an initial aberration is applied and an image is recorded. The Fourier transform and spectral density of the image are then calculated and the appropriate range

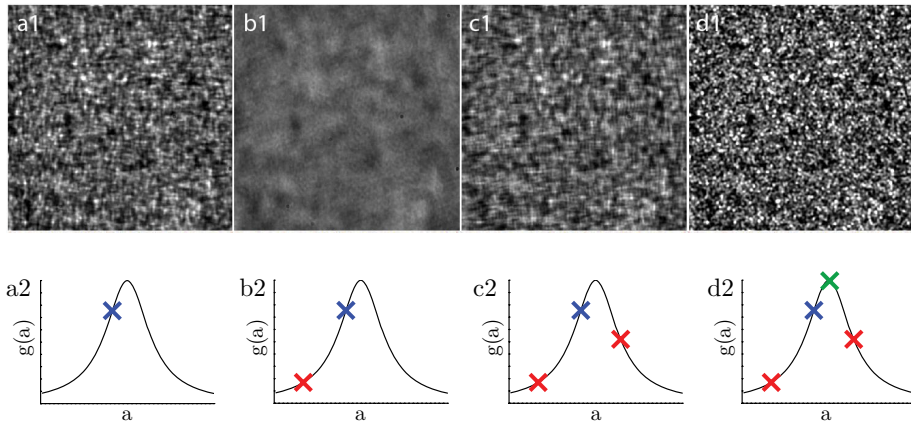


Figure 9: Correction of a single Lukosz aberration mode (astigmatism,  $i = 5$ ) for a scatterer specimen and using low spatial frequencies. The first row shows the raw images of the specimen and the second row illustrates schematically the sampling of the Lorentzian curve used in the optimization calculation. (a1 & a2) correspond to an arbitrary initial aberration of magnitude, (b1 & b2) have an additional negative bias while (c1 & c2) have an additional positive bias of equal magnitude. (d1 & d2) show the corrected image calculated with the parabolic minimization. Image after [14].

of frequency components are summed, giving the metric measurements. The same procedure is repeated with both negative and positive aberrations (i.e. stronger and weaker aberrations), resulting in two additional metric measurements, indicated by the red and blue crosses in Figure 9 a2, b2, and c2. Due to the parabolic maximum of the Lorentzian, the maximum can be calculated from as little as three measurements (indicated by the green cross in Fig. 9 d2 and the correction is then applied to the DM. To correct multiple modes, each modal coefficient is measured in the same manner before the full correction aberration containing all modes is applied. While this technique is based only on low spatial frequencies, it is shown that both low and high frequency components can be effectively corrected. In all the cases investigated, a Strehl ratio greater than 0.8, close to the diffraction limit, was obtained. This indicates that, when aberration statistics are unknown, choosing small spatial frequencies for an initial correction is a reasonable strategy. If further correction is required, they can be performed using a larger range of frequencies. *Debarre et al.* concluded that this correction scheme is largely independent of the object structure and proposed this approach also to be valid for coherent or partially coherent systems.

### 3.1.3 Structured Illumination Microscopy

It is often desired for biological samples to produce clear images of focal planes deep within a thick sample (i.e. optical sectioning) and common techniques include point-scanning techniques such as confocal or multiphoton techniques which are described in section 3.2.

Widefield techniques such as Structured Illumination (SI) microscopy can also provide optical sectioning. However, the sectioning is realized using a standard microscope, an incoherent light source and without the need for a scanning mechanism. For SI microscopy, a grid is imaged into the specimen to produce a one-dimensional sinusoidal excitation pattern in the focal plane. The resulting sinusoidal fluorescence image, consisting of both in-focus and out-of-focus fluorescence emission, is then normally recorded. Several images are taken, each corresponding to a different grid position equivalent to three different phase shifts of the grating. The grid pattern only appears in the focal plane while it is blurred in the out-of-focus regions. Hence, it is possible to extract an optical section from the spatially modulated component of the images via a simple calculation.

Based on the SI microscopy technique presented by *Neil et al.* in 2005 [29] as well as their earlier work on indirect wavefront sensing using a conventional microscope [14] in 2007 (described in the previous

section), *Debarre et al.* combined both techniques in 2008 and proposed an AO scheme for use in SI microscopy [26].

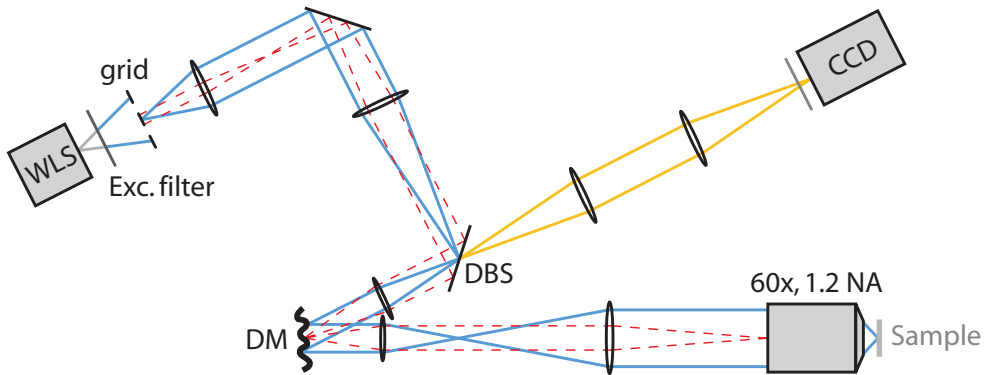


Figure 10: Experimental setup for structured illumination microscopy with aberration correction. WLS - white light source, DM - deformable mirror, DBS - dichroic beamsplitter. The blue rays mark the illumination path; the detection path is shown in yellow. Image after [26] .

They again presented a sensorless wavefront detection scheme, which is shown in Fig. 10. The method to obtain the aberration correction is similar to the one presented and explained in the previous section, and will not be described again. The results of the implemented AO scheme is shown in Fig. 11 for aberration correction on a fluorescent mouse intestine. The image contrast and sharpness improvement is clearly visible in the image 11b compared to the uncorrected image in 11a. As a result of the aberration correction, and as shown in Fig. 11c, the contrast of small sample features (blue arrows) is better defined after (red solid line) rather than before (black dotted line) correction.

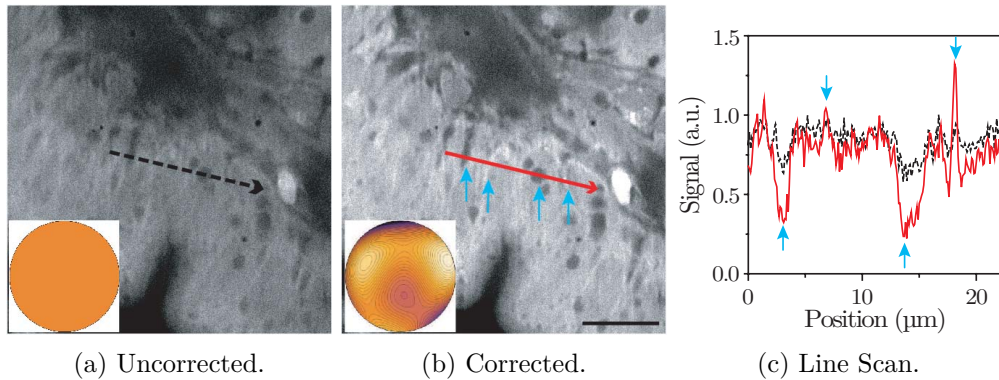


Figure 11: Aberration correction in structured illumination microscopy. A fluorescent mouse intestine sample was imaged (a) without, (b) with aberration correction with inserts showing the phase induced by the deformable mirror. (c) Profile along the lines drawn on the images, both profiles normalized so that their mean value is identical. As a result of the resolution improvement, the contrast of small sample features (blue arrows) is better defined after (red solid line) rather than before (black dotted line) correction. The imaging depth was approximately 10  $\mu\text{m}$ , scale bar size 10  $\mu\text{m}$ . Image after [26].

The authors also explained an additional benefit of aberration correction for structured illumination microscopy. The adaptive element can also be used to improve the rejection of the out-of-focus fluorescence. When imaging thick specimen, noise fluctuations in the fluorescence signal between the three successive widefield images obtained for the maximization process result in a large out-of-focus background in the calculated sectioned images. Since this background arises from fluorescence generated outside the focal plane, it is not sensitive to the presence of aberrations. By applying large aberrations the grid pattern is suppressed and only the out-of-focus noise can be measured. By subtracting this aberrated image from the original sectioned image, the fluorescent background can be efficiently

removed, leading to greatly improved contrast of the in-focus structures.

In conclusion, the authors presented a sophisticated, easy to implement and highly versatile AOM scheme which allowed for aberration correction induced by the optical system, the specimen or the focus depth. While the presented scheme used a widefield microscope, *Debarre et al.* were also optimistic that similar AO methods based on indirect, image based aberration detection could be applied to point-scanning methods.

### 3.2 Point Scanning Microscopes

Just as with the widefield techniques, adaptive optics quickly found its way into point scanning techniques to improve the image and signal quality. Scanning methods are useful for imaging biological specimens, since they can provide high resolution imaging in three-dimensions. Illumination is usually provided by a laser that is focused into the sample. The light emitted or reflected from the specimen is collected, usually through the same objective lens, and its intensity is measured by a detector. Since this only provides information about the intensity at a single spot, the focal point is then scanned through the specimen and point-by-point the image is acquired.

This section will give a brief description how AO is applied to HG, CARS and STED microscopy. Following this will be a more detailed analysis of how adaptive optics is implemented into confocal (section 3.2.1) and multi-photon fluorescence microscopes (section 3.2.2 and 3.2.3).

Adaptive optics techniques have been developed for all common point scanning microscopes. Using both the second- and third-harmonic intensity signals as the optimization metric for an indirect wavefront sensing scheme, *Jesacher et al.* [30] as well as *Olivier et al.* [31] showed AO applied to higher harmonic generation microscopy. The aberration correction is compensating both system- and specimen-induced aberrations when imaging live mouse embryos. The authors demonstrated an improved signal level and resolution, with peak intensity increased by almost *unit[50]%* and the FWHM decreased by 14 % to 1.22  $\mu\text{m}$  compared with a value of 1.15  $\mu\text{m}$  for a non-aberrated system.

Even better results were reported by *Wright et al.* [25] when applying AO to CARS. The authors achieved a signal improvement by a factor of 3 for samples at a depth of 700  $\mu\text{m}$  and a factor of 6 for muscle tissue at a depth of 260  $\mu\text{m}$ . Their completely random optimization typically converged after 3000 changes mirror shapes. With a mirror speed of up to 1 kHz this is sufficiently fast. The approach is well suited to CARS microscopy where photobleaching does not occur but is less applicable for other microscopy techniques.

It is also possible to apply AO to Stimulated Emission Depletion (STED) microscopy (see [32] for basic working principle of STED) as recently presented by *Gould et al.* [33], again employing an indirect sensing scheme. Using a phase mask, the authors both created the doughnut shape depletion beam and simultaneously implemented an aberration correction. Using an additional spatial light modulator, aberration correction is also implemented in the excitation beam. The correction in the depletion beam leads to a better resolution while the correction of the excitation beam path results in a stronger signal and less noise. Unlike many other indirect sensing methods, here the image brightness proved to be a poor quality metric due to the depletion. Hence the authors introduced a new metric that seeks to optimize both image brightness and image sharpness in a combined approach. The new approach worked successfully resulting in a  $\tilde{5}$ -fold increase in the peak signal as well as a  $\tilde{3.2}$ -fold improvement in resolution.

#### 3.2.1 Confocal Microscopes

The confocal microscopy can operate in reflection or fluorescence mode. Both are a dual pass system, which means that both the illumination path and the emission path have to be corrected in an AO confocal microscope. The first attempt to apply AO in confocal microscopy was done by *Martin J. Booth et al.* [34]. They implemented indirect wavefront sensing to a confocal fluorescence microscope in a closed-loop way. Aberration measurement and correction was done sequentially. First a preset positive bias aberration was introduced by a deformable membrane mirror. An image was taken and all of its pixel values were summed and averaged to give the value of  $W_1$ . Then, it was added to the

system the equivalent negative bias aberration, obtaining  $W_2$ . They had shown before that the value of the difference signal,  $W = W_1 - W_2$ , is approximately proportional to the amount of the Zernike mode  $Z_i$  present in the sample. They applied this procedure for several different Zernike modes, updating the mirror shape each time. A simple representation of the experimental set-up is shown in Fig. 12. With this sequential method for correcting aberrations they achieve a 1.8 times smaller axial PSF, using two cycles of this modal wavefront sensor applied to low order aberration modes.

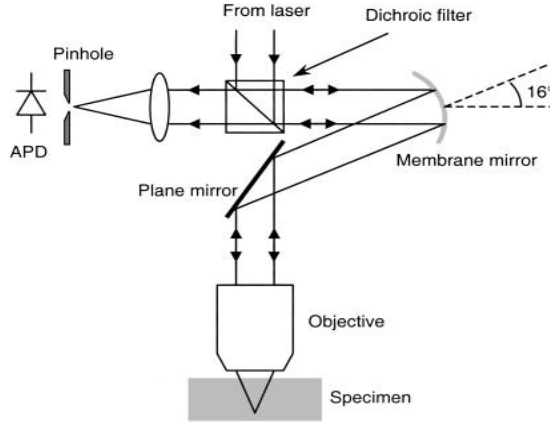


Figure 12: The illumination beam was passed through a beam expander and reflected by the membrane mirror such that the angle between the incident and reflected beams was  $16^\circ$ . Then it passed into the objective lens focusing the light into the specimen. Fluorescence light from the specimen was collected by the same objective. In this configuration, the membrane mirror can compensate for aberrations introduced into both the illumination and emission optical paths.

A different way to apply AO in confocal microscopy was presented by *Xiaodong Tao et al* [35]. They used a direct wavefront sensor in a fluorescence confocal microscope. Particularly, they implemented a Shack-Hartmann sensor with fluorescent microspheres ( $1\text{ }\mu\text{m}$  diameter) embedded in the sample as a point source reference beacons. Their setup was designed to operate in a close-loop. The corrector device was a deformable mirror. A separate laser channel was added to excite the microsphere, which shared the same light path with the imaging channel. The results showed a  $4.3 \times$  improvement in the Strehl ratio and a 240 % improvement in the signal intensity for fixed mouse tissues at depths of up to  $100\text{ }\mu\text{m}$ . Although the effects of these microspheres in the live tissue have to be further investigated, this direct method enabled a shorter exposure time during sensing and a higher speed of imaging, which showed its potential ability for live *in vivo* imaging.

### 3.2.2 Indirect Wavefront Sensing in Multiphoton Scanning Microscopy

Its intrinsic optical sectioning, larger penetration depth, reduced photo damage as well as other advantages allowed nonlinear microscopy in general, and Two-Photon Fluorescence Microscopy (TPFM) in particular, to become a very important tool in biological imaging since its first presentation by *Denk et al.* in 1990 [36]. As with most AO microscopy techniques, both a direct and indirect wavefront sensing scheme can be deployed for the use with TPFM. Indirect sensing using a model based optimization was already explained (section 2.2) and presented (section 3.1 in detail). *Marsh et al.* presented the first and fairly simple indirect sensing approach, correcting only for depth induced aberrations as early as 2003 [37]. Again, based on their earlier works ([14, 26]), *Débarre et al.* presented another highly sophisticated application of their image based wavefront sensing scheme in 2009 [27]. Since both *Marsh* and *Débarre* essentially used the standard TPFM setup and the image optimization is very similar to the one presented earlier, we will not describe these methods here again. *Rueckel et al.* presented a wavefront correction method using coherence-gated wavefront sensing [12] which is beyond the scope of this report.

For two-photon fluorescence microscopy, it is not essential to correct for sample or system induced

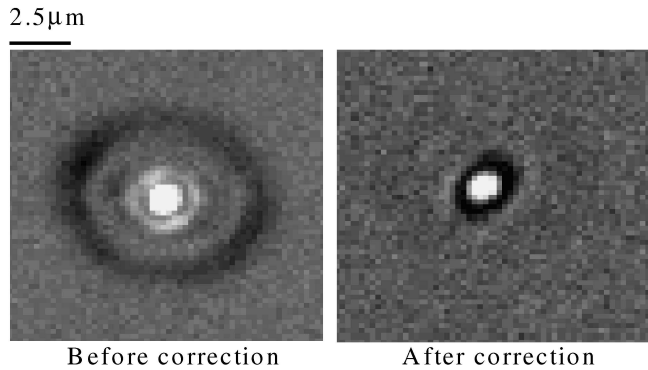


Figure 13: Normalized CCD image of two-photon fluorescence at a focus depth of 600  $\mu\text{m}$  with and without correction with the DM. [39]

aberrations on the collected beam. Since it is a point scanning technique, all the light emitted in the focus region is collected and only the relative intensity difference is important for the generation of the image (see [38] for a detailed review on TPFM). To achieve the highest possible resolution, especially when imaging deep in a tissue, it is however very important to correct aberrations of the excitation beam. This will not only result in a better, i.e. smaller focus spot, but will also highly increase the efficiency of the nonlinear process. As described in earlier sections, an indirect wavefront sensing is usually applied for microscopic applications, and such a system developed by *Sherman et al.* [39] and based on a genetic optimization algorithm will be presented in this section. To overcome some of the inherent disadvantages of indirect sensing, *Aviles-Espinosa et al.* developed a direct sensing scheme for two-photon fluorescence microscopy which will be described in section 3.2.3.

In multiphoton microscopy, the excitation of the sample by a high power, ultra short pulses is typically quadratic or cubic. If a diffraction limited spot is created in the focus of the laser beam, the generated nonlinear signal will have a maximum and hence signal intensity is a good image quality metric for these methods. Using a genetic optimization algorithm to maximize the nonlinear signal, *Sherman et al.* [39] present a indirect sensing scheme for multiphoton microscopy correcting depth induced aberrations efficiently. Corrections were made with a genetic learning algorithm using the two-photon fluorescence intensity feedback to determine the desired shape for a deformable mirror. *Albert et al.* [18] were the first to investigate possible advantages of GA over random search algorithms in 2000. There, genetic algorithms were used for correcting off-axis aberrations in beam-scanning confocal microscopy, increasing the usable scan area by a factor of 9. Other adaptive optics methods using GA soon followed, optimizing fiber coupling efficiency [40] or optimizing harmonic conversion efficiency [41]. These methods however were not directly related to microscopy. It was *Sherman et al.* who presented a better application of GA in microscopy, efficiently correcting for depth-induced spherical aberration and off-axis aberrations, providing full adaptive aberration compensation over a 3D volume. For simplicity, the authors used a Coumarin water solution in place of the biological sample that is commonly analyzed with multiphoton fluorescence microscopy. The long working distance objective allowed the scanning from the surface of the cover glass up to 2 mm into the sample. The aberration correction is achieved by running the genetic algorithm to determine the DM wavefront that would best maximize the two-photon intensity at the focus as measured by the fluorescence power. An optimum DM solution emerged after as little as 10 generations, resulting in a measurement time of approximately three minutes. This aberration correction can then be saved for future use, as long as the objective is the same and the location of the DM in relation to the microscope has not been changed. The first proof of an improvement in the image quality was done qualitatively by simply taking an image of the two-photon fluorescence as shown in Fig. 13. Since no biological sample is present, the imaged signal should ideally be a diffraction limited spot and hence the imaged points directly represent the lateral point spread function. The corrected image therefore shows a significant improvement in image quality.

To quantify their results, *Sherman et al.* scanned the laser focus spot along the longitudinal axis of a quartz/Coumarin-water interface. Third harmonic signals were generated at that interface and their

signal intensity was used to measure the longitudinal PSF. The normalized longitudinal PSF as shown in Fig. 14a reflects the normalized PSF decrease in FWHM from  $14.6 \mu\text{m}$  to  $8.1 \mu\text{m}$  with adaptive correction at a focus depth of  $450 \mu\text{m}$ . The most significant result of correction is exemplified by the un-normalized longitudinal PSF shown in Fig. 14b. Whereas the normalized PSF shows the decrease in FWHM due to the combination of spherical bias and DM correction, in contrast to operation with no bias and no correction, the un-normalized longitudinal PSF shows a remarkable improvement in third harmonic intensity by a factor of more than 7 that results from compensating the spherical aberration.

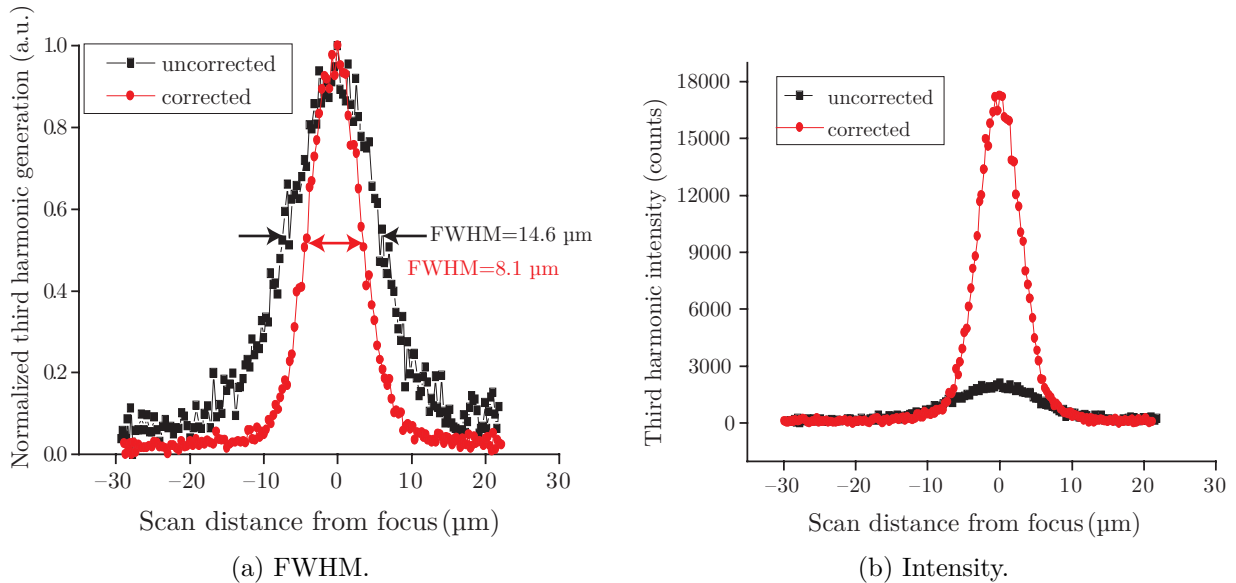


Figure 14: Normalized longitudinal point spread for focusing depth of  $450 \text{ mm}$  for both corrected and uncorrected showing increase in resolution due to correction, as well as un-normalized showing increase in intensity due to correction [39].

### 3.2.3 Direct Wavefront Sensing in Two Photon Fluorescence Microscopy

As described in section 2.1 and 3.1.1, to be able to use a wavefront sensor, one needs a point like reference source which is then used to detect the aberrations. This point like source can be artificially created and embedded in the sample. However, it might cause damage to the sample or might influence the behavior of living samples, limiting its potential for *in vivo* imaging. *Aviles-Espinosa et al.* realized that two-photon excited fluorescence naturally produces a small confined volume that emits incoherently, thus it can be used as the guide-star. The setup presented by the authors is basically an inverted microscope, modified to be used as laser scanning TPFM (see paper for detailed component description and working principle). A mode locked Ti:sapphire laser ( $\lambda = 810 \text{ nm} \& 860 \text{ nm}$ , pulse duration =  $100 \text{ fs}$ , repetition rate =  $80 \text{ MHz}$ , average powers in sample plane =  $1.5 \text{ mW}$  to  $5.6 \text{ mW}$ ) is used as the excitation beam. The wavefront sensing is performed using a Shack-Hartmann Wavefront Sensor (SH WFS), located at one of the output ports of the microscope. The aberration correction is realized with an electromagnetic Deformable Mirror (DM). The authors investigated the performance of their AOM system using both *Caenorhabditis elegans* and mouse brain samples. For small aberrations and weak scattering only a modest improvement in signal intensity was shown. At an imaging depth of  $25 \mu\text{m}$ , the measured signal enhancement was  $1.75\times$  by correcting the coupling aberrations, and  $3.61\times$  when focusing aberrations were corrected as well. Similar values were obtained imaging deeper into the tissue. *Caenorhabditis elegans* tissue scatterers only weakly and hence spherical aberration is the main aberration for imaging deep into the tissue. Since these should be easily corrected using the presented scheme, the authors were surprised by these relatively small improvements in the signal quality. By using an additional agar pad to simulate moderate scattering as well as imaging deeper into the tissue, the authors investigated the correction efficiency further. Deep into the sample ( $127 \mu\text{m}$ ) where large sample induced aberrations are prominent, improvements of the signal intensity by a factor of  $22.59\times$

were possible, as shown in Fig. 15. It is noteworthy, that the aberration correction increases the signals local maxima while the local minima remain unaltered.

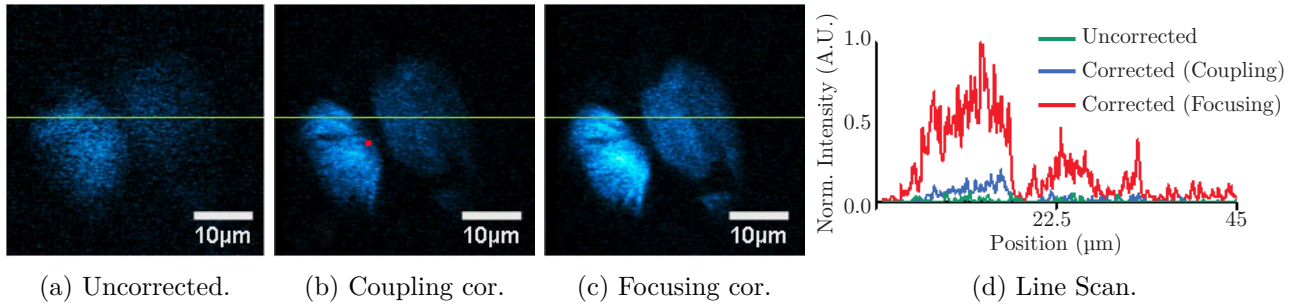


Figure 15: In vivo *C. elegans* sample imaged at 127  $\mu\text{m}$  depth. (a) shows the uncorrected image of a worm section, (b) displays the same section with coupling correction applied and (c) shows the section when both coupling and focusing aberrations are corrected. (d) shows the intensity profile along the green line in the images for all three correction cases. The correction of coupling aberrations improves the signal intensity by a factor of only 1.94 whereas the correction of both coupling and focusing aberrations results in a very good improvement of 22.59. Image after [42].

Finally, the authors investigated the AO system performance using strongly scattering mouse brain tissue. They showed that a correction is still possible, but it is less efficient than for moderately scattering samples. It is furthermore possible to record aberration corrected images with a single exposure, no need for complex optimization algorithms and without further sample preparation (i.e. no fluorescent microspheres need to be inserted). This minimize photobleaching effects, photo-toxicity and limits negative effects to the living sample. Since no model is needed to correct the aberrations, the method is robust and can be applied to fixed and in vivo biological samples. An overall intensity improvement of more than one order of magnitude was shown in some cases. In conclusion, the authors presented a flexible and versatile application of adaptive optics in microscopy which can be used in wide range biological imaging applications where a high resolution is required.

## 4 Conclusion & Future Prospects

While adaptive optics has been applied in many fields for more than fifteen years, in biological imaging it is still a relatively new system. Since new AO techniques for modern microscopes are just being developed, it will take more time before AO can become a standard component of laboratory microscopes.

It is important to remark that AO applied to microscopy does not overcome the diffraction limit but rather helps to restore a diffraction limited imaging case. It therefore usually yields in an improvement in both axial and lateral resolution as well as an increase in signal intensity. In other words, AO extends the capabilities of high-resolution or superresolution techniques, especially extending the ability to image deeper into tissue. The advantages of correcting aberrations always depend on the specimen under study and the microscopy technique used. One of the most critical issues in AO applied to microscopy is the accuracy in the sensing process, that is, how we obtain the aberration information from the sample. It seems to be that indirect sensing is the first option in almost all the experiments for AO microscopes. This is because it is easier to implement in microscopy since it only requires a deformable mirror and no point-like emitter is needed. Indirect sensing is however usually slower than direct sensing.

An important drawback in most AO methods for microscopy is the relatively slow wavefront detection. As long as aberrations don't change quickly or when just considering a small region of a sample, this is not a problem. However, when imaging larger parts of a sample or when trying to image fast processes in live samples, AO techniques are often slow. Thus, it is important to further optimize the current systems or to develop a completely new, faster correction devices (using multiple correctors be-

ing a possible solution). This would extend the ability to correct aberrations in real time and with less exposure of the specimens during the measurement. The slow sensing is also an important drawback for aberration correction in an industrial microscope used in hospitals or biological labs. Thorlabs offers a ready-made adaptive optics system for TPFM [43] but it also aims at research labs and is not suitable for the end user. Big microscope manufacturers like Zeiss and Leica have not yet presented a single commercial microscope using adaptive optics, even though Zeiss owns a patent on the technology [44]. Furthermore, AO methods have not been implemented in techniques such as STORM and PALM yet. First publications in these fields are only a matter of time and are probably due to the young age of the methods, as AO techniques are currently being developed [45].

It is difficult to give specific advice regarding the choice of the correct adaptive optics system. If measurement speed and photobleaching are a concern, direct sensing should be considered, with the possible downside of a higher complexity and the need for a guide star. If a maximal signal intensity is more important, photobleaching is not a problem and if space, hardware and budget are limited, indirect sensing might be the better choice. It offers a cheap and easy AO implementation if time is not a concern or if suitable optimization algorithms can be developed. In the end, the right choice has to be determined based on the microscopy technique and system constraints. Despite all this, further improvements in the sensing and correction process will certainly further extend the already wide range AO applications in modern microscopes in the future.

## References

- [1] M. J. Booth. *Adaptive Optics in Microscopy*, pp. 295–322. Wiley-VCH Verlag GmbH & Co. KGaA. ISBN 9783527635245 (2011). URL <http://dx.doi.org/10.1002/9783527635245.ch14>.
- [2] H. W. Babcock. “The possibility of compensating astronomical seeing.” *Pub. Astron. Soc. Pacific* (Oct 1953). vol. 65. URL <http://dx.doi.org/10.1086/126606>.
- [3] L. N. Thibos. “Principles of hartmann-shack aberrometry.” *Vision Science and its Applications* (2000). URL <http://www.opticsinfobase.org/abstract.cfm?URI=VSIA-2000-NW6>.
- [4] B. C. Platt & R. Shack. “History and principles of shack-hartmann wavefront sensing.” *Journal of refractive surgery* (Oct. 2001). vol. 17(5). URL <http://view.ncbi.nlm.nih.gov/pubmed/11583233>.
- [5] I. Weingaertner & M. Schulz. “Interferometric methods for the measurement of wavefront aberrations.” *Proc. SPIE* (1993). vol. 1781:pp. 266–279. URL <http://dx.doi.org/10.1117/12.140978>.
- [6] M. J. Booth. “Wavefront sensorless adaptive optics for large aberrations.” *Opt. Lett.* (Jan 2007). vol. 32(1):pp. 5–7. URL <http://dx.doi.org/10.1364/OL.32.000005>.
- [7] M. J. Booth, D. Débarre et al. “Adaptive optics for biomedical microscopy.” *Opt. Photon. News* (1 2012). vol. 23(1):pp. 22–29. URL <http://dx.doi.org/10.1364/OPN.23.1.000022>.
- [8] F. Zernike. “Beugungstheorie des schneidenverfahrens und seiner verbesserten form, der phasenkontrastmethode.” *Physica* (1934). vol. 1(7–12):pp. 689 – 704. URL [http://dx.doi.org/10.1016/S0031-8914\(34\)80259-5](http://dx.doi.org/10.1016/S0031-8914(34)80259-5).
- [9] R. Tyson. *Adaptive Optics Engineering Handbook (Optical Science and Engineering)*. CRC Press, 1 edn. (11 1999). ISBN 9780824782757.
- [10] J. Porter, H. Queener et al. *Adaptive Optics for Vision Science: Principles, Practices, Design and Applications (Wiley Series in Microwave and Optical Engineering)*. Wiley-Interscience, 1 edn. (7 2006). ISBN 9780471679417.

- [11] D. Malacara, editor. *Optical Shop Testing (Wiley Series in Pure and Applied Optics)*. Wiley-Interscience, 3 edn. (7 2007). ISBN 9780471484042. URL <http://dx.doi.org/10.1002/9780470135976>.
- [12] M. Rueckel, J. A. Mack-Bucher et al. “Adaptive wavefront correction in two-photon microscopy using coherence-gated wavefront sensing.” *Proceedings of the National Academy of Sciences* (2006). vol. 103(46):pp. 17137–17142. URL <http://dx.doi.org/10.1073/pnas.0604791103>.
- [13] O. Azucena, J. Crest et al. “Wavefront aberration measurements and corrections through thick tissue using fluorescent microsphere reference beacons.” *Opt. Express* (Aug 2010). vol. 18(16):pp. 17521–17532. URL <http://dx.doi.org/10.1364/OE.18.017521>.
- [14] D. Debarre, M. J. Booth et al. “Image based adaptive optics through optimisation of low spatial frequencies.” *Opt. Express* (6 2007). vol. 15(13):pp. 8176–8190. URL <http://dx.doi.org/10.1364/OE.15.008176>.
- [15] J. R. Fienup & J. J. Miller. “Aberration correction by maximizing generalized sharpness metrics.” *J. Opt. Soc. Am. A* (Apr 2003). vol. 20(4):pp. 609–620. URL <http://dx.doi.org/10.1364/JOSAA.20.000609>.
- [16] A. J. Wright, D. Burns et al. “Exploration of the optimisation algorithms used in the implementation of adaptive optics in confocal and multiphoton microscopy.” *Microscopy Research and Technique* (2005). vol. 67(1):pp. 36–44. URL <http://dx.doi.org/10.1002/jemt.20178>.
- [17] J. Li & H. Chen. “A closed-loop adaptive optical system based on genetic algorithm.” In “Electrical and Control Engineering (ICECE), 2010 International Conference on,” (2010) pp. 16–18. URL <http://dx.doi.org/10.1109/iCECE.2010.12>.
- [18] O. Albert, L. Sherman et al. “Smart microscope: an adaptive optics learning system for aberration correction in multiphoton confocal microscopy.” *Opt. Lett.* (Jan 2000). vol. 25(1):pp. 52–54. URL <http://dx.doi.org/10.1364/OL.25.000052>.
- [19] D. Whitley. “A genetic algorithm tutorial.” *Statistics and Computing* (1994). vol. 4(2):pp. 65–85. URL <http://dx.doi.org/10.1007/BF00175354>.
- [20] M. Booth. “Wave front sensor-less adaptive optics: a model-based approach using sphere packings.” *Opt. Express* (Feb 2006). vol. 14(4):pp. 1339–1352. URL <http://dx.doi.org/10.1364/OE.14.001339>.
- [21] W. Lukosz. “Der einfluß der aberrationen auf die optische Übertragungsfunktion bei kleinen ortsfrequenzen.” *Optica Acta: International Journal of Optics* (1963). vol. 10(1):pp. 1–19. URL <http://dx.doi.org/10.1080/713817744>.
- [22] W. H. Press, S. A. Teukolsky et al. *Numerical Recipes 3rd Edition: The Art of Scientific Computing*. Cambridge University Press, 3 edn. (9 2007). ISBN 9780521880688. URL <http://www.nr.com/>.
- [23] M. Schwertner, M. Booth et al. “Characterizing specimen induced aberrations for high na adaptive optical microscopy.” *Opt. Express* (12 2004). vol. 12(26):pp. 6540–6552. URL <http://dx.doi.org/10.1364/OPEX.12.006540>.
- [24] V. N. Mahajan. *Optical Imaging and Aberrations, Part II. Wave Diffraction Optics (SPIE Press Monograph Vol. PM209)*. SPIE Press, 2 edn. (8 2011). ISBN 9780819486998. URL <http://dx.doi.org/10.1117/3.898443>.
- [25] A. J. Wright, S. P. Poland et al. “Adaptive optics for enhanced signal in cars microscopy.” *Opt. Express* (12 2007). vol. 15(26):pp. 18209–18219. URL <http://dx.doi.org/10.1364/OE.15.018209>.

- [26] D. Débarre, E. J. Botcherby et al. “Adaptive optics for structured illumination microscopy.” *Opt. Express* (6 2008). vol. 16(13):pp. 9290–9305. URL <http://dx.doi.org/10.1364/OE.16.009290>.
- [27] ——. “Image-based adaptive optics for two-photon microscopy.” *Opt. Lett.* (8 2009). vol. 34(16):pp. 2495–2497. URL <http://dx.doi.org/10.1364/OL.34.002495>.
- [28] O. Azucena, J. Crest et al. “Adaptive optics wide-field microscopy using direct wavefront sensing.” *Opt. Lett.* (Mar 2011). vol. 36(6):pp. 825–827. URL <http://dx.doi.org/10.1364/OL.36.000825>.
- [29] M. A. A. Neil, R. Juskaitis et al. “Method of obtaining optical sectioning by using structured light in a conventional microscope.” *Opt. Lett.* (Dec 1997). vol. 22(24):pp. 1905–1907. URL <http://dx.doi.org/10.1364/OL.22.001905>.
- [30] N. Olivier, D. Débarre et al. “Dynamic aberration correction for multiharmonic microscopy.” *Opt. Lett.* (10 2009). vol. 34(20):pp. 3145–3147. URL <http://dx.doi.org/10.1364/OL.34.003145>.
- [31] A. Jesacher, A. Thayil et al. “Adaptive harmonic generation microscopy of mammalian embryos.” *Opt. Lett.* (10 2009). vol. 34(20):pp. 3154–3156. URL <http://dx.doi.org/10.1364/OL.34.003154>.
- [32] S. W. Hell & J. Wichmann. “Breaking the diffraction resolution limit by stimulated emission: stimulated-emission-depletion fluorescence microscopy.” *Opt. Lett.* (Jun 1994). vol. 19(11):pp. 780–782. URL <http://dx.doi.org/10.1364/OL.19.000780>.
- [33] T. J. Gould, D. Burke et al. “Adaptive optics enables 3d sted microscopy in aberrating specimens.” *Opt. Express* (9 2012). vol. 20(19):pp. 20998–21009. URL <http://dx.doi.org/10.1364/OE.20.020998>.
- [34] M. J. Booth, M. A. A. Neil et al. “Adaptive aberration correction in a confocal microscope.” *Proceedings of the National Academy of Sciences* (4 2002). vol. 99(9):pp. 5788–5792. URL <http://dx.doi.org/10.1073/pnas.082544799>.
- [35] X. Tao, B. Fernandez et al. “Adaptive optics confocal microscopy using direct wavefront sensing.” *Opt. Lett.* (Apr 2011). vol. 36(7):pp. 1062–1064. URL <http://dx.doi.org/10.1364/OL.36.001062>.
- [36] W. Denk, J. Strickler et al. “Two-photon laser scanning fluorescence microscopy.” *Science* (1990). vol. 248(4951):pp. 73–76. URL <http://dx.doi.org/10.1126/science.2321027>.
- [37] P. Marsh, D. Burns et al. “Practical implementation of adaptive optics in multiphoton microscopy.” *Opt. Express* (5 2003). vol. 11(10):pp. 1123–1130. URL <http://dx.doi.org/10.1364/OE.11.001123>.
- [38] M. Oheim, D. J. Michael et al. “Principles of two-photon excitation fluorescence microscopy and other nonlinear imaging approaches.” *Advanced Drug Delivery Reviews* (2006). vol. 58(7):pp. 788 – 808. URL <http://dx.doi.org/10.1016/j.addr.2006.07.005>.
- [39] L. Sherman, J. Y. Ye et al. “Adaptive correction of depth-induced aberrations in multiphoton scanning microscopy using a deformable mirror.” *Journal of Microscopy* (2002). vol. 206(1):pp. 65–71. URL <http://dx.doi.org/10.1046/j.1365-2818.2002.01004.x>.
- [40] F. Gonté, A. Courteville et al. “Optimization of single-mode fiber coupling efficiency with an adaptive membrane mirror.” *Optical Engineering* (2002). vol. 41(5):pp. 1073–1076. URL <http://dx.doi.org/10.1117/1.1466462>.
- [41] P. Villoresi, S. Bonora et al. “Optimization of high-order harmonic generation by adaptive control of a sub-10-fs pulse wave front.” *Opt. Lett.* (Jan 2004). vol. 29(2):pp. 207–209. URL <http://dx.doi.org/10.1364/OL.29.000207>.

- [42] R. Aviles-Espinosa, J. Andilla et al. “Measurement and correction of in vivo sample aberrations employing a nonlinear guide-star in two-photon excited fluorescence microscopy.” *Biomed. Opt. Express* (Nov 2011). vol. 2(11):pp. 3135–3149. URL <http://dx.doi.org/10.1364/BOE.2.003135>.
- [43] Thorlabs. “Two-photon microscope with adaptive optics demonstration.” URL <http://bit.ly/IAx50m>. Visited on 12/11/13.
- [44] R. Wolleschensky, R. Grub et al. “Applications of adaptive optics in microscopy.” (August 2004). URL <http://www.freepatentsonline.com/6771417.html>.
- [45] A. Jasaitis, G. Clouvel et al. “Extreme precision in 3d: Adaptive optics boosts super-resolution microscopy.” URL <http://bit.ly/1cQri59>. Visited on 2/12/13.